Macromolecules
ARTICLE

Macromolecules **2010**, *43*, 10621–10627 **10621**
DOI: 10.1021/ma101767f

Spatiotemporal Evolution in Morphogenesis of Thermoreversible Polymer Gels with Fibrillar Network

Che-Min Chou and Po-Da Hong*

Department of Materials Science and Engineering, National Taiwan University of Science and Technology, Taipei, 10607, Taiwan

Received August 3, 2010; Revised Manuscript Received November 5, 2010

ABSTRACT: A scattering modeling approach is used to clarify the formation of the thermoreversible polymer gel with a fibrillar network. We find that the gelation has to do with the spatiotemporal evolution of the so-called "coherent structure"—the nonlocalized, fibril nucleation via the fluctuation instability and fibril growth coupled with a cooperatively coarsening concentration wave—and is a direct consequence of the spinodal crystallization far from equilibrium in the solution. The present result rejects the common opinion that the gelation is nothing more than the percolation problems and poses an interesting question about the entropy-driven crystallization.

1. Introduction

Thermoreversible polymer gels are often considered to be a percolating network formed through physical association of long-chain molecules.[1−5] Further, one can make the jump from the junction structure to the network properties, because no characteristic mesostructure is a consequence of the self-similarity of the percolating network. This view explains why, except for the rheology,[6] the experiments[7,8] over recent decades always remain on the microstructure in terms of the classification proposed by Flory[9] and de Gennes.[10] However, the frequently observed diverse, hierarchical morphologies have proved that the polymer gelation is not that simple right from the start.[11−14]

Is the thermoreversible gelation nothing more than a percolation problem? Recent researches on the colloid gels[15] and the low-molecular gelators[16−18] have suggested that the gelation can arise from some self-organizing/assembling processes driven by phase transitions—*not really percolating*. Interestingly, some experimentalists have presumed somewhat similar mechanism in polymer systems in spite of no enough evidence.[19] While all seem to question the universality of the percolation theory, there should not be any ambiguity in the answer. For variety gel systems, many theorists go a long way to give an exact description of their universality class in phase transitions.[3−5] The idea behind the percolation theory has a very intrinsic problem. Namely, the gelation as a critical phenomenon, the theory expects a well-defined sol−gel "phase" boundary in the equilibrium phase diagram.[20,21] On the other hand, a new problem upraises: if the thermoreversible polymer gels are taken out from the percolation universality class, where will they belong? Hence, we contend that a more precise experiment, based on tracing the morphogenesis, is needed to identify the most important factor for the polymer gelation.

Forming a fibrillar network is a very widespread phenomenon in the polymer gels and the low-molecular gelators. It is accepted for the gelators that the fibrillar structure is due to the crystalline fibril branching[17,18] and may be depicted by the solidification.[22] Naturally, this seems logical for polymer, because the crystallization does occur in most polymer gels.[6−8] However, a similar observation does not automatically guarantee a similar origin and process. The solidification has no thought for the entanglement complexity of polymers, not to mention the fact that the mechanism does not by itself expect—*how does the topological connectivity occur?* Obviously, the crux lies in how the fibril growth brings the topological connectivity on the mesoscale.

There are two mechanisms for the thermoreversible gelation with fibril structure. One is the bond percolation by fibril junctions (a typical phase transformation in polymer solutions); another is the self-organization/assembly by fibril aggregation/evolution (an nonequilibrium phenomenon). However, the experiments based upon equilibrium thermodynamics are not possible to tell which one is most nearly in agreement with the fact. Thus, we proposed a judgment. If the gelation is characterized by the fibril nucleation covering over the entire transient network instantaneously (i.e., the bonding probability depends only on the nucleation kinetics), it is a percolation process; if not, it relies on when and how do the molecular topological entanglement pin the self-organizing/assembling processes. Tracing the evolving fibrils by the depolarized small-angle light scattering (*d*-SALS) technique can provide an access to model the system in questions.[23] In this paper, we use a qualitatively reliable *full-scattering-pattern* analysis to perform a systematic stepwise survey of the gelation process.[24,25] By reconstructing the whole process, the present work would not only answer how the fibrils self-organize into the network but also clarify what the nature of the morphogenesis in that process is.

2. Experimental Methods

2.1. Materials. The fibrillar network was prepared by syndiotactic polystyrene (s-PS) (syndiotactic content of over 99.9%, $M_w = 2 \times 10^5$, $M_w/M_n = 2.8$, Idemitsu Petroleum Co. Ltd.) dissolved in *o*-xylene, and then by quenching the homogeneous solution ($C = 0.5$ g dL^{-1}) from 408 K to the gelation temperature 323 K.

2.2. Scanning Electron Microscopy. The freeze-dried network was prepared as follows: the homogeneous s-PS/*o*-xylene solution was quenched from 408 to 323 K for 1 day to form a wet gel, and then the wet gel was placed into the freeze-drying equipment (Emitech Ltd., K775X Turbo Freeze-Dryer with LN_2 Fed Cold Stage) at 138 K. Under a vacuuming condition (1×10^{-5} mBar)

*Corresponding author. E-mail: poda@mail.ntust.edu.tw. Fax: +886-2-27376544.

Published on Web 11/30/2010

for more than 1 day, the freeze-dried network was obtained. The morphology of the freeze-dried network was investigated by scanning electron microscopy (SEM; Hitachi S-3000N).

2.3. Time-Resolved *d*-SALS. The optical arrangement of the apparatus has been described previously.[23] A 5 mW polarized He−Ne laser was used as the incident source, and the polarization direction of the beam was adjusted by a half-wave plate. The beam was then spatially filtered, expanded, and shined onto the sample. The sample cell was placed on the temperature controlled stage (Linkam Scientific Co., THMS-600), and the scattered light intensity was directly imaged through the Fourier lens and an analyzer onto the CCD camera (Apogee Instruments Inc., Alta U2000 CCD camera). The digitized images were transferred the real-time processing to a personal computer. In present study, the reliable data are about scattering angle $\theta = 0.87-21.5°$, corresponding to $q = 0.22-5.57\ \mu m^{-1}$.

2.4. Time-Resolved FT-IR. The time-resolved infrared spectrum was measured at a resolution of 1 cm^{-1} with a Nicolet 6700 FT-IR Spectrometer (Thermo Fisher Scientific Inc.). The s-PS/*o*-xylene solution was enclosed in a HT-32 heated demountable cell with 0.5 mm path length spacer inserted between two KBr windows. The crystal form of the s-PS fibril is δ phase with a 2_1 helical conformation corresponding to a regular TTG^+G^+ sequence,[26] and the conformational-sensitive band of the sequence is at 572 cm^{-1};[26−28] thus, the wavenumber range scanned was set to 568−576 cm^{-1} to trace the band.

3. Results

3.1. Scattering Modeling of the Fibrillar Network. Figure 1a shows the SEM micrograph and the corresponding depolarized scattering pattern of the s-PS/*o*-xylene gel. As shown in Figure 1b, left, sketch, the network can be modeled as the rigid fibrillar skeleton connected by the soft entangled junction. In the common practice of the *d*-SALS experiment, the structural identification of the scatterers is accomplished by comparison with theoretical form scattering, like the Murakami et al. anisotropic rod model.[29] As shown in Figure 1b, right, the theoretical pattern (the rod length $L = 5\ \mu m$) is similar to the experimental one, but the length estimation differs markedly from the SEM observation (ca. 1 μm). Undoubtedly, the present pattern should be richer in structure. In early works,[30] it is implicitly assumed that the structure scattering can be excluded from *d*-SALS. Later, we knew that the structural information does exist and can be extracted by our scattering modeling approach.[24,25]

For the scattering from an evolving hierarchical structure, giving the explicit analytical form of the scattering pattern is rather difficult or even impossible. Instead, the scattering modeling is a compromising phenomenological approach which can lead to a better understanding of the interrelation/interaction between scatterers at different timing and hierarchy during the process. Before building a realistic model, we would like to define two terms: form factor and structure factor. The form factor is the scattering intensity for a scatterer alone and is related to the shape and scattered ability of it. The structure factor is scattering intensity for the interference of the scatterers and is referred to the spatial arrangement of them. Besides, the form factor also describes the scatterers' level in the hierarchical structure. If the density−density correlation functions of two structures have the convolution relationship,[31,32] the sub one names as the form factor. Let us return to our main subject. Considering many crystalline fibrils create a topological connectivity and then show a highly correlated evolution. The model needs two form factors to define the fibrils and their correlation; one more structure factor is needed to characterize the large-scale inhomogeneities of the network, as shown in Figure 1c.

Two mechanisms were considered: the *fibril aggregation/branching* and the *fluctuation coupling*. The former is not new[13,18] and holds for the following case, as shown in Figure 2 top. First, either an aggregate or a branching object requires "an" origin,[18] and the fractal characteristic should be detected and analyzed. Second, if the cluster is formed by the aggregation, it will be a two-stage process, i.e., the fibril growth and then aggregation. In the present study, however, no fractal was observed, and the fibrils grew to join one another as a continuous process. Hence, a new fluctuation coupling mechanism goes as follows: the "growing" fibrils are spread out and embedded in nonlocalized concentration waves posed by them. As shown in Figure 2 bottom, in addition to the fibril form factor (Murakami et al.'s model), the Debye−Bueche *fluctuation* model[33] as another form factor provided a suitable formalism to describe the fibrils' correlation. By its very nature, the Debye−Bueche model is often used to analyze the spatial inhomogeneity and makes no reference to the correlation between the discrete fibrils. Nevertheless, just these fibrils give rise to mesoscopically observable inhomogeneity. Given such a "mixing," the scattered intensity should be expressed by the sum of these two terms. Furthermore, because of a polymer chain inevitably participating in several fibrils, as the fibril growth, the topological entanglement would join the fibrils up. So we treated the structure factor as a loose assembly of such fibril

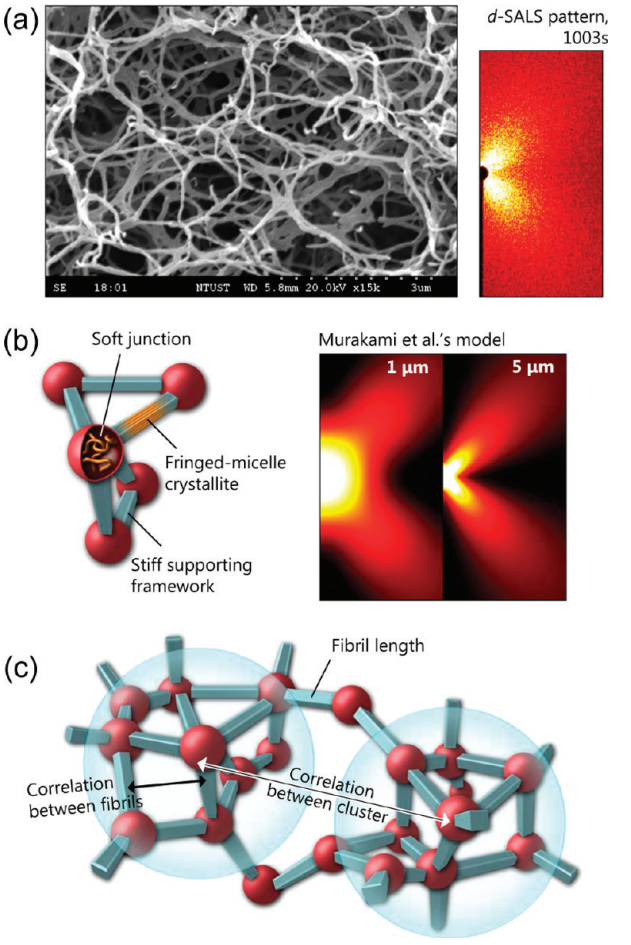

Figure 1. (a) SEM micrograph (left) and the representative half-depolarized scattering pattern (right) of the fibrillar network, prepared by 0.5 g dL^{-1} s-PS/*o*-xylene solution at 323 K. (b) Left: the sketch of the fibrillar skeleton. Right: the theoretical patterns of the crystalline fibril by Murakami et al.'s model[29] for different fibril lengths ($L = 1$ and 5 μm). The parameters used are the anisotropies of the fibril $\delta = 1$, the polar angle of the rod axis $\omega_0 = 0°$, and the refractive index of the medium $m_1 = 1.503$. (c) Hierarchical structure of the fibrillar network.

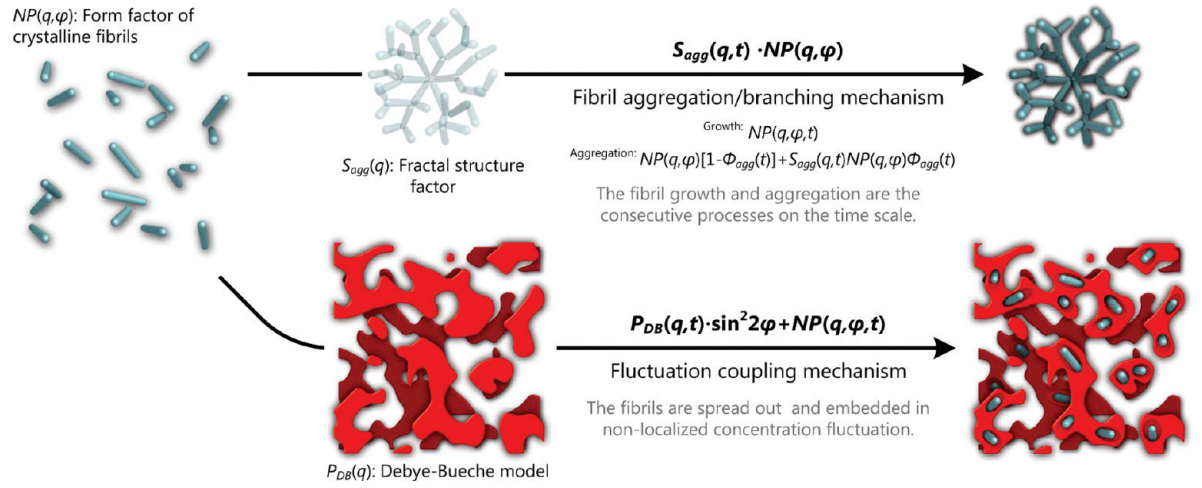

Figure 2. Scattering modeling of the fibrillar network.

clusters/domains. The model is then given by

$$I_{Hv}(q,\varphi) = S(q)[NP_{Hv}^{Rod}(q,\varphi) + P_{DB}(q)\sin^2 2\varphi] \quad (1)$$

where $I_{Hv}(q,\varphi)$ is the depolarized scattered intensity (where q is the scattering vector, and φ is the azimuthal angle), $S(q) = 1 - \beta e^{-(\gamma\xi_s q)^2}$ is the structure factor of the spatial correlation between each cluster (where ξ_s is the correlation length, and β and γ are the amplitude and the range of the correlation, respectively),[13] N is the number of the fibrils, $P_{Hv}^{Rod}(q,\varphi) = (k\pi L\delta/4)^2[p_2(\cos\omega_0)]^2\ \tilde{P}\ (qL,\varphi)$ is the form factor of the crystalline fibril given by the Murakami et al.'s model [where k is related to the absolute intensity, L is the fibril length, δ is the anisotropies of the fibril, ω_0 is the polar angle of the fibril axis, $p_2(x)$is the second order Legendre function, and $\tilde{P}(qL,\varphi)$ is the scaled form factor],[29] $P_{DB}(q) = 4\pi K\xi_{DB}^3\langle\eta_{DB}^2\rangle/(1 + q^2\xi_{DB}^2)^2$ is the Debye−Bueche factor (where K is a constant, ξ_{DB} is the Debye−Bueche correlation length, and $\langle\eta_{DB}^2\rangle$ is the mean-square fluctuation),[33] and $\sin^2 2\varphi$ is the "optical transmission" property of the analyzer from the scattering matrix theory.[34,35]

The model consists of 11 parameters (i.e., constants k, K, ω_0, γ, and δ; time-dependent parameters N, L, β, ξ_s, ξ_{DB}, and $\langle\eta_{DB}^2\rangle$). How to better determine their values is a problem, especially in an absolute intensity fitting. However, for a semiquantitative analysis, we set $K = 1$ and $\delta = 1$, and combined k and N to be a floating intensity coefficient in the fitting. In the Murakami et al.'s model, if the polymer in the fibril has a helical conformation, the angular dependence of the d-SALS pattern is independent of ω_0;[29] thus we set $\omega_0 = 0°$. The structure factor, γ, is given by

$$\gamma = \frac{1}{2\sqrt{\pi}}\sigma^{-1}$$

where σ is the ratio of the cluster size to their average distance (if $\sigma = 1$, the clusters are closely packed; if $\sigma < 1$, the clusters are close but not in contact; if $\sigma > 1$, the clusters overlap).[13] Considering the loose assembly of the clusters,$\sigma < 1$ seems to be reasonableness; thus we set $\sigma = 0.67$ ($\gamma = 0.42$). For the remainder time-dependent parameters, formally, there may be not just one solution but a range, corresponding to "one" scattering pattern (two-dimensional, space case). The validity of the modeling is limited to the selection of these parameters, because the results may reflect in part the way in which those were selected. Nevertheless, it is possible with appropriate constraints during analysis, like refer to the real-space SEM micrograph. On the other hand, one must not forget that we face a spatiotemporal evolution (three-dimensional case); only the physical clarity of these solutions appears to be continuous on the time scale and can thus represent a "right" answer. Figure 3 shows that the modeling results agree well with the experimental patterns—even including the background.

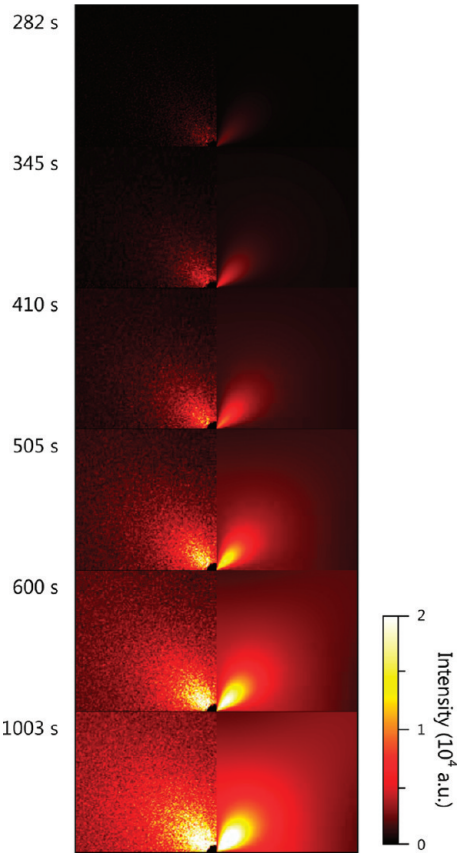

Figure 3. A comparison of the experimental (left half, a series of quarter patterns) and the best-fitted theoretical (right half) scattering patterns.

3.2. Morphogenesis of Self-Organizing Network. Figure 4 is plotted to test the dynamical scaling of the scattering function. The combined form factors should fall onto a single master curve when the Debye−Bueche term just reflects the spatial correlations of the fibrils themselves. Interestingly, the scaled scattering functions were not found to be time-independent

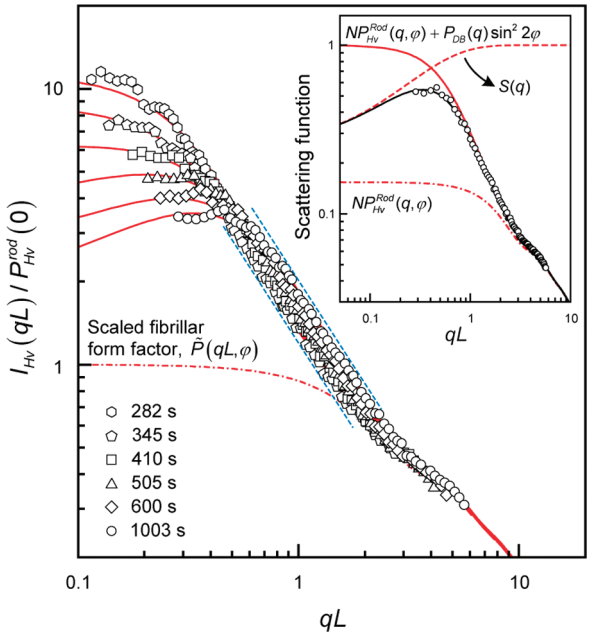

Figure 4. Reduced scattering functions (φ = 45°) of our fibrillar network model. The solid lines are the base-fitted theoretical scattering function, and the dash-dot line is the scaled form factor of the fibril by Murakami et al.'s model. The inset shows the behavior and interaction between three scattering factors.

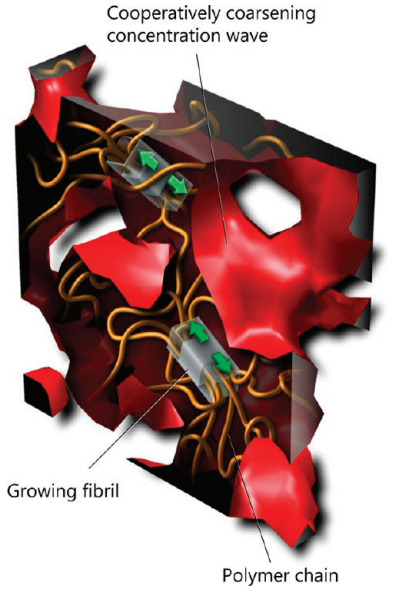

Figure 5. Schematic representation of the coherent structure.

but were slightly shifted toward high qL. The asynchronous behavior implies that the "individual" Debye−Bueche fluctuation, as a cooperatively coarsening concentration wave, was "coherent" with the growing fibrils. Figure 5 depicts the so-called coherent structure. On the other hand, as time goes on, the scaled intensity decreased and developed a peak indicating the emergence of distinct fibrils and definite network from the fluctuation background.

Although the gelation obviously had to do with the coherent structure evolution, how the fluctuation is coupled with the fibril growth was still unanswered. What is its origin? Assuming a thermal fluctuation in the initial homogeneous background, its wavelength, if related to the coupling, should be close to ξ_{DB} at the fibril nucleation. We can use the

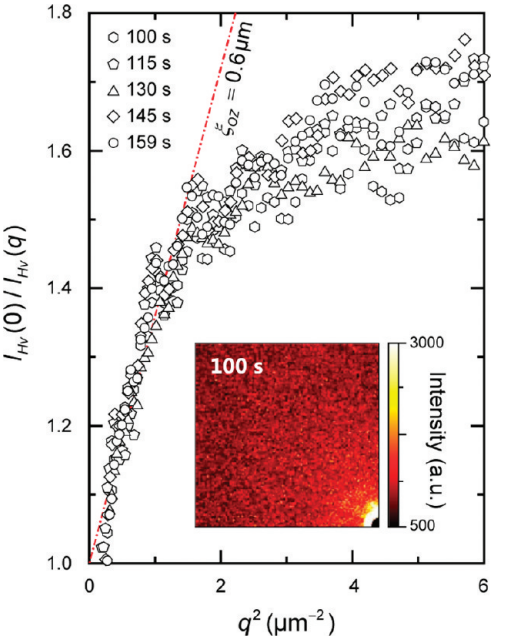

Figure 6. Ornstein−Zernike plot of the data for the initial background scattering and the speckle pattern.

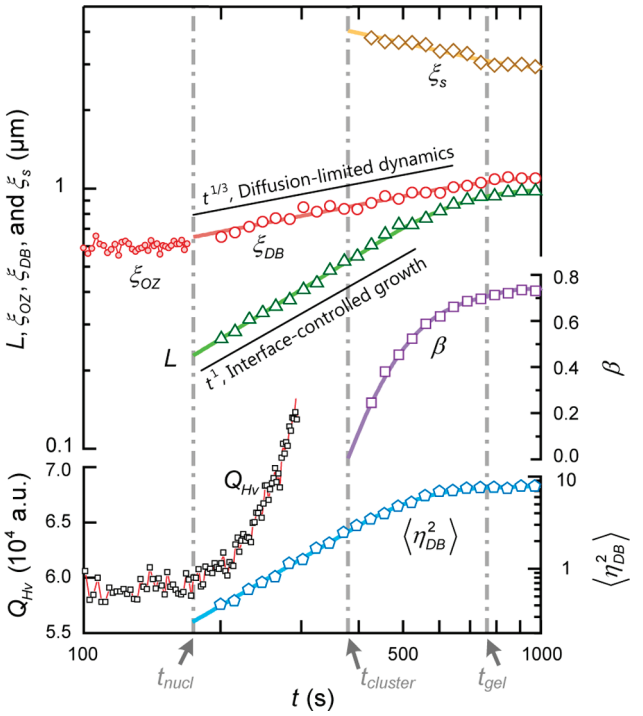

Figure 7. All scattering modeling parameters from a systematic stepwise survey of time-resolved scattering patterns.

Ornstein−Zernike equation $I(q) = I(q = 0)(1 + q^2\xi_{OZ}^2)^{-1}$ to test whether such background fluctuation exists.[31] Figure 6 shows the Ornstein−Zernike plot and the speckle pattern before the fibril nucleation. The point to observe is that the characteristic fluctuation length-scale (~0.5 μm) was also shown in other polymer gel systems.[36−41] This would be considered later.

Figure 7 shows the result of a systematic stepwise survey of the time-resolved scattering patterns. At first glance, the process was classified into four regimes: (i) the fluctuation stage ($t < t_{nucl}$, where t_{nucl} is the nucleation time defined by

the remarkable change in the scattering invariant, $Q_{Hv} = \int_0^\infty I_{Hv}(q,\varphi = 45°)\, q^2\, dq$); (ii) the coherent evolution stage ($t_{nucl} < t < t_{cluster}$, where $t_{cluster}$ is the onset of connecting between the growing fibrils defined by $\beta \rightarrow 0$); (iii) gelation stage ($t_{cluster} < t < t_{gel}$, where t_{gel} is the gelation time determined experimentally by the fluidity observed); (vi) aging stage ($t > t_{gel}$). As expected, ξ_{DB} tended smoothly toward ξ_{OZ} at t_{nucl}. This convergence implies that a triggering source as a thermal fluctuation with a band of specific wavelengths was needed to generate the polymer fibrillar network. In other words, given such the characteristic fluctuation in the initial background, the subsequent nucleation and growth of the fibrils then amplified the fluctuation so that the network emerged gradually. In the coherent evolution stage, the increase of $\langle \eta_{DB}^2 \rangle$ and the diffusion-limited dynamics $\xi_{DB} \sim t^{1/3}$ confirmed that the evolution depended on the "uphill" diffusion like the intermediate-stage spinodal decomposition.[42] While, the interface-controlled growth $L \sim t^1$ indicated that there was no need for long-range diffusion around the growth front of the embedded fibrils, for their dynamics became local. Ultimately, with the fibril growth the topological connectivity appeared and led to the heterogeneous network (see Figure 7, β and ξ_s). Here, we also noticed that $L(t = t_{gel}) \approx \xi_{OZ}$ was interesting in that it shows that the initial fluctuation not only triggered the coherent structure but also, to a large extent, predetermined the final fibrillar skeleton.

4. Discussion

4.1. Comparison with the Previous Opinion. From a phase transition point of view, the experimentalists attempt to answer the origin of the polymer fibrillar network.[36−41, 43−45] A fundamental understanding of the thermodynamics, the kinetics, and the mechanism of the gelation is therefore of great importance. However, recent studies on thermodynamic equilibrium microstructures (junctions) and morphologies (networks)[6−8] and on global kinetics[43−45] do not fill the gap in our knowledge on the formation mechanism. Some experiments have been carried out in order to search for the factors controlling the microstructures and morphologies.[36−41] The point is that the gelation is due to the competition−cooperation between the crystallization and the phase separation in the polymer solution. Namely, the process is initiated via the spinodal decomposition and subsequent crystallization in the bicontinuous polymer-rich phase.[39,40] The main evidence comes from analyzing the wide-angle light scattering (WALS) data of the early stage concentration fluctuations in terms of Cahn's spinodal theory.[46] While there can be no doubt about the existence of the fluctuation, we divide on the relevance of the mechanism.

First, the extrapolation spinodal point determined in Cahn's way is kinetic, but whether the thermodynamic miscibility gaps are precisely those observed in kinetic experiment is a problem.[36−41] Second, the light scattering peak provides access to an analysis of the spinodal structure at each evolution stage—fluctuation, transition, and coarsening,[47] but no observed spinodal structure may be questionable. In a number of experiments, especially those time trace observed by the WALS,[36−41] the crystallization/gelation intervenes at the fluctuation stage of the spinodal decomposition, leading to a "physical pinning." Such the pinning effect retains the initial fluctuation structure (wavelength $\sim 0.5\,\mu$m) in the final gel morphologies which coincidentally agrees with our observation in section 3.2. Clearly, even though the early stage fluctuation is approximately described by Cahn's spinodal theory, its formation might be of a rather different origin. Now that our "coherent" picture could rationalize the previous observation, we might argue that the complex concept of the competition-cooperation of the multiphase transitions are not required in order to explain the experimental data presented.

4.2. When Does the Coherent Structure Occur? We may safely assume that its condition is related to L_c (the critical length of the fibril nucleus) and ξ_{OZ}, which give a criterion when combined with the intrinsic persistence length of the polymer, p, as $p < L_c < \xi_{OZ}$. When $L_c \gg \xi_{OZ}$, the details of the fluctuation do not matter, and then the "classical" crystalline nucleus forms and grows locally. If $L_c < \xi_{OZ}$, the nucleating fibrils seem roughly equivalent to the diffuse nucleus of Cahn and Hilliard's nonclassical nucleation theory[48,49] or the wave packet of Binder and Stauffer's cluster-dynamics approach.[50] The two "non-classical" pictures would perhaps explain why the Cahn's spinodal theory can self-consistently describe the early stage fluctuation observed by the previous WALS experiments. Pursuing further the cause of the coherence drives us to the problem about the spinodal crystallization in bulk polymers.[51−53] The situation shows some similarity to the coherent structure formation presented here. In Ryan et al.'s SAXS experiment[51](also see Kaji et al.[52]), they found a fluctuation-induced anomalous scattering at the early stage crystallization which implies the observation of a spontaneous fluctuation process rather than a sudden nucleation event. By taking into account an additional correlation effect induced by topological entanglement of polymers, Muthukumar's kinetic model gives a reasonable overall account of Ryan et al.'s disputed data.[53] In his model, the nucleation instability is embodied in the "intrinsic" properties of polymers, but the way is in fact ignoring the general metastable character of the polymer crystallization. As we see it now, the Muthukumar model may be inappropriate or at least incomplete. In view of this, let us then consider another possibility: whether under certain circumstances, the "extrinsic" fluctuations can be strong enough to vanish the metastability and then the spinodal crystallization can occur.

Recent studies have noted that the metastability limit can be realistic in supercooled liquids, if the system has strongly viscoelastic effects.[54,55] Cavagna et al.'s viscoelastic nucleation theory[54] gives a *kinetic spinodal* temperature which marks the relaxation time of the supercooled liquid exceeding the nucleation time of the crystal. Considering a mapping between the relaxation time and the length scale ($\tau \sim \xi^2$), we analogueize to have a criterion $L_c \approx \xi_{OZ}$ in which the limit exists. We can summarize the main ideas—if the critical nucleus size corresponds to the characteristic wavelengths of the initial fluctuation, or the nucleation time takes place fairly close to the relaxation time of the polymer disentanglement, the spinodal crystallization occurs and the coherent structure is formed. At this point, our coherence criterion could be regarded as a signature of the gradual transition from the classical crystallization to the spinodal crystallization.

4.3. Hypothesis of Entropy-Driven Crystallization. Just like pattern-forming phenomena in dissipative systems,[56,57] the gelation was via the fluctuation instability, and the *initial* fluctuation predetermined the *final* morphology. We may wonder what "small effects" felt by polymer molecules induce such a self-organizing process. Let us draw attention to the conformational change of the s-PS during the fluctuation stage, as shown in Figure 8a. The integrated IR intensity of the regular TTG^+G^+ conformation emerged immediately after quenching, increased linearly before any indication of forming observable fibrils ($t < t_{nucl}$), and approached only asymptotically the gelation stage. Superficially, this observation

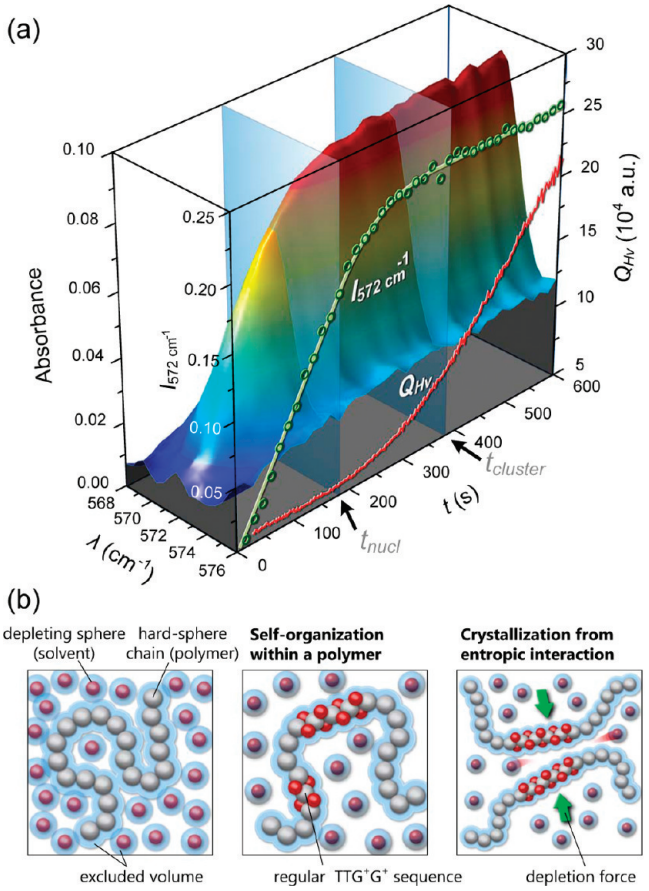

Figure 8. (a) Real-time trace of the conformational-sensitive IR band of the regular TTG^+G^+ sequence of the s-PS (572 cm^{-1}) in the early stage nucleation. (b) Entropy-driven crystallization in the polymer solution. Left: The excluded volume effect leads to a crowded environment, and the maximum of the conformational entropy leads to an inaccessible region or a closed chain loop to confine the degree of translational freedom of the solvent molecules (the depleting spheres). Middle: The solvents act as "side chain" affixed to the hard-sphere chain to stabilize the self-organizing helix, thus favoring the global maximum of the system's entropy. Right: Again, the free-volume per depleting sphere is larger in the ordered (the crystal) than in the disordered (the self-organizing helix) phase.

seems to agree: whereas the polymer crystal is partially built up with the intramolecular periodic structure, when a polymer molecule is possible to self-organize into the regular sequence, the next "crystallization" through intermolecular packing of these sequences must proceed in a more *continuous* and *collective* fashion as the "spinodal" process.[58]

However, two deep questions should be addressed. First, what does drive the self-organization within a polymer molecule? Second, why does the solution show up as a long-lived metastable state, despite its fluctuation instability? The answers to both questions may lie in understanding how the s-PS chain behaves in the solution. Nevertheless, the instability in the solution itself causes the experimental difficulties. To avoid the problem, the comparable atactic polystyrene (a-PS, $M_w = 2.116 \times 10^5$, $M_w/M_n = 1.01$, Sigma-Aldrich Inc.) was used as a substitute [the intrinsic viscosity $[\eta]$, which characterizes the hydrodynamic specific volume of a polymer coil, is 0.69 dLg^{-1} and the Huggins constant, which is related to the structure of polymer coil (for the self-avoiding chains, $k < 0.52$), is 0.488]. Inasmuch as the two polymers are the stereoisomers, their behaviors should be essentially identical at least at $t = 0$. Unexpectedly, in the present condition, the gelation occurred at $[\eta]C = 0.345$ (much lower than the hydrodynamic overlapped concentration, $[\eta]C \sim 1$)! Obviously, the formation of the self-organized helix (i.e., the regular TTG^+G^+ sequence of the s-PS) accompanied the significant expansion of the s-PS coils and made gelation at the dilute situation. From Daniel et al.,[27] the self-organizing helix can be stabilized by *o*-xylene molecules intercalated between the phenyl groups (the π—π interactions[59]). It, however, seems rather doubtful that all was driven entirely by such a "chemical" force. On the other hand, we were concerned as to why the coil expansion is not an *instantaneous* conformational transition but again a *continuous* process.

From a different angle, we all know that the preferred polymer crystal is the chain-folded lamellar crystal.[60] The chain-folding not only is a most efficient way of packing polymer chains but also satisfies the homogeneous nucleus and the sharp interface as required for the classical nucleation theory. In contrast, the fibril, a so-called "fringed-micelle crystal," could collapse due to the high cumulative strain energy[61] and the entropy effect of overhanging loose chains at the sterically nervous transition-interface-layers. Thus, in bulk crystallization, the fibril is forbidden on the kinetic grounds.[61,62] However, the fibril nucleation during the gelation is certainly a different physical process. Now that the fibril structure does not favor the minimization of the interface energy, the global entropy maximization may be the primary in its formation. Indeed, using the hard-sphere chain model, the Prigogine−Flory−Patterson theory[63] predicts the entropy-driven phase separation to occur when the loss in the mixing entropy is compensated by the translational entropy increment.[64,65] Snir and Kamien also show that a purely entropic force can be enough to bend the stiff polymer into a helix.[66] So we suggest a hypothesis of entropy-driven crystallization to understanding the fibril formation. Figure 8b illustrates how this may arise.

We first consider a hard-sphere chain (self-avoiding chain) surrounded by many depleting spheres (solvent molecules). The excluded volume of the hard-sphere chain reduce the free volume in which the depleting spheres may live, as shown in Figure 8b, left. Clearly, the only way to heighten the spheres' free volume (translational entropy) at constant internal energy is to allow the significant expansion of the hard-sphere chain, while its conformational entropy is more or less lost. However, whether the translational entropy can have an appreciable effect on the expansion of the hard-sphere chain should depend on the polymer concentration. We predict that the maximum translational entropy could be obtained near the overlap threshold ($[\eta]C \sim 1$), enough to outweigh the loss in the conformational entropy. Even so, the stability of the expanded hard-sphere chain still has to depend on its persistence time. The stabilization can be done in two ways: either by a higher activation energy barrier for the rotational isomerization, or by the special chemical forces such as the π−π interactions, as shown in Figure 8b, middle. Furthermore, as the self-organizing helices grow beyond certain critical length, the depletion attraction caused by them would be sufficiently large to induce the fluctuation instability, as shown in Figure 8b, right. We finally know why the solution shows up as the long-lived metastable state.

5. Conclusions

This study has demonstrated that the morphogenesis of the polymer fibrillar network, in fact, begins with the nonlocalized spinodal crystallization far from equilibrium, continues with the evolution of the coherent structure, and ends with the emergence of the topological connectivity. All results reject the common opinion. So we argue that the thermoreversible gelation needs to

be reconceptualized for the future development of the field. In place of the percolation model, the jamming—a "new" perspective—is a good point which depicts a nonequilibrium fluid (sol)-solid (gel) transitions due to the sudden arrest of particle or molecule dynamics.[66−69] To conclude, the polymer fibrillar network should be regarded as a fibrillar-like, polycrystalline off-equilibrium configuration which is frozen into a permanent state by the jamming of polymer chains.[70,71] On the other hand, with the intricate phenomena uncovered partly, understanding how the entropy behaves seems to be emerging immediately. Although these call for further investigation, the present findings are enough to kindle interest in reexamining the origin of the mesoscopic complexity of soft matters.

Acknowledgment. We thank Y. W. Ye for her help with raw data collections. This work was supported by the NSC of the Taiwan under Contract NSC- 98-2221-E-011-009-MY3.

References and Notes

(1) Coniglio, A.; Stanley, H. E.; Klein, W. *Phys. Rev. Lett.* **1979**, *42*, 518.
(2) Stauffer, D.; Coniglio, A.; Adam, M. *Adv. Polym. Sci.* **1982**, *44*, 103.
(3) Adam, M.; Lairez, D. In *Physical Properties of Polymer Gels*; Cohen Addad, J. P., Ed.; John Wiley & Sons: New York, 1996; Chapter 4.
(4) De Gennes, P. G. *J. Phys., Lett.* **1976**, *37*, L1.
(5) Stauffer, D. *J. Chem. Soc., Faraday Trans. 2* **1976**, *72*, 1354.
(6) Te Nijenhuis, K. *Thermoreversible Networks: Viscoelastic Properties and Structure of Gels*; Springer: New York, 1997.
(7) Guenet, J. M. *Thermoreversible Gelation of Polymer and Biopolymer*; Academic Press: New York, 2002.
(8) Keller, A. *Faraday Discuss.* **1995**, *101*, 1.
(9) Flory, P. J. *Faraday Discuss. Chem. Soc.* **1974**, *57*, 7.
(10) De Gennes, P. G. *Scaling Concept in Polymer Science*; Cornell University Press: New York, 1985.
(11) Kanaya, T.; Takeshita, H.; Nishikoji, Y.; Ohkura, M.; Nishida, K.; Kaji, K. *Supramol. Sci.* **1998**, *5*, 215.
(12) Hirokawa, Y.; Okamoto, T.; Kimishima, K.; Jinnai, H.; Koizumi, S.; Aizawa, K.; Hashimoto, T. *Macromolecules* **2008**, *41*, 8210.
(13) Ferri, F.; Greco, M.; Arcòvito, G.; de Spirito, M.; Rocco, M. *Phys. Rev. E* **2002**, *66*, 011913.
(14) Chou, C. M.; Hong, P. D. *Macromolecules* **2004**, *37*, 5596.
(15) Lu, P. J.; Zaccarelli, E.; Ciulla, F.; Schofield, A. B.; Sciortino, F.; Weitz, D. A. *Nature* (*London*) **2008**, *453*, 499.
(16) Weiss, R. G.; Terech, P. *Molecular Gels: Materials with Self-Assembled Fibrillar Networks*; Springer: Dordrecht, The Netherlands, 2006.
(17) Douglas, J. F. *Langmuir* **2009**, *25*, 8386.
(18) Raghavan, S. R. *Langmuir* **2009**, *25*, 8382.
(19) Guenet, J. M. *J. Rheol.* **2000**, *44*, 947.
(20) Tanaka, T.; Swislow, G.; Ohmine, I. *Phys. Rev. Lett.* **1979**, *42*, 1556.
(21) Heermann, D. W.; Stauffer, D. *Z. Phys. B* **1981**, *44*, 339.
(22) Gránásy, L.; Pusztai, T.; Börzsönyi, T.; Warren, J. A.; Douglas, J. F. *Nat. Mater.* **2004**, *3*, 645.
(23) Chou, C. M.; Hong, P. D. *Macromolecules* **2003**, *36*, 7331.
(24) Chou, C. M.; Hong, P. D. *Macromolecules* **2008**, *41*, 6540.
(25) Chou, C. M.; Hong, P. D. *Macromolecules* **2008**, *41*, 6147.
(26) Guerra, G.; Musto, P.; Karasz, F. E.; MacKnight, W. J. *Makromol. Chem.* **1990**, *191*, 2111.
(27) Daniel, C.; Deluca, M. D.; Guenet, J. M.; Brûlet, A.; Menelle, A. *Polymer* **1996**, *37*, 1273.
(28) Kobayashi, M.; Kozasa, T. *Appl. Spectrosc.* **1993**, *47*, 1417.
(29) Murakami, Y.; Hayashi, N.; Hashimoto, T.; Kawai, H. *Polym. J.* **1973**, *4*, 452.
(30) Stein, R. S.; Rhodes, M. B. *J. Appl. Phys.* **1960**, *31*, 1873.
(31) Higgins, J. S.; Benoît, H. C. *Polymers and Neutron Scattering*; Oxford University Press: Oxford, U.K., 1994.
(32) Kerker, M. *The Scattering of Light and Other Electromagnetic Radiation*; Academic: New York, 1969.
(33) Debye, P.; Bueche, A. M. *J. Appl. Phys.* **1949**, *20*, 518.
(34) Desborder, M.; Meeten, G. H.; Navard, P. *J. Polym. Sci., Part B: Polym. Phys.* **1989**, *27*, 2037.
(35) Van de Hulst, H. C. *Light Scattering by Small Particles*; John Wiley & Sons: New York, 1957.
(36) Kawanish, K.; Takeda, Y.; Inoue, T. *Polym. J.* **1986**, *18*, 411.
(37) Matsuo, M.; Tanaka, T.; Ma, L. *Polymer* **2002**, *43*, 5299.
(38) Matsuo, M.; Miyoshi, S.; Azuma, M.; Bin, Y.; Agari, Y.; Sato, Y.; Kondo, A. *Macromolecules* **2005**, *38*, 6688.
(39) Takeshita, H.; Kanaya, T.; Nishida, K.; Kaji, K. *Macromolecules* **1999**, *32*, 7815.
(40) Hong, P. D.; Chou, C. M. *Macromolecules* **2000**, *33*, 9673.
(41) Takeshita, H.; Kanaya, T.; Nishida, K.; Kaji, K. *Macromolecules* **2001**, *34*, 7894.
(42) Bailey, A. E.; Poon, W. C. K.; Christianson, R. J.; Schofield, A. B.; Gasser, U.; Prasad, V.; Manley, S.; Segre, P. N.; Cipelletti, L.; Meyer, W. V.; Doherty, M. P.; Sankaran, S.; Jankovsky, A. L.; Shiley, W. L.; Bowen, J. P.; Eggers, J. C.; Kurta, C.; Lorik, T., Jr.; Pusey, P. N.; Weitz, D. A. *Phys. Rev. Lett.* **2007**, *99*, 205701.
(43) Ohkura, M.; Kanaya, T.; Kaji, K. *Polymer* **1992**, *33*, 5044.
(44) Dikshit, A.; Nandi, A. K. *Macromolecules* **1998**, *31*, 8886.
(45) Hong, P. D.; Chou, C. M. *Polymer* **2000**, *41*, 8311.
(46) Cahn, J. W. *J. Chem. Phys.* **1965**, *42*, 93.
(47) Hashimoto, T. In *Structure and Properties of Polymers*; Thomas, E. L., Ed.; Wiley-VCH: New York, 1993; Chapter 6.
(48) Cahn, J. W.; Hilliard, J. E. *J. Chem. Phys.* **1958**, *28*, 258.
(49) Cahn, J. W.; Hilliard, J. E. *J. Chem. Phys.* **1959**, *31*, 688.
(50) Binder, K.; Stauffer, D. *Rep. Prog. Phys.* **1987**, *50*, 783.
(51) Ryan, A. J.; Fairclough, J. P. A.; Terrill, N. J.; Olmsted, P. D.; Poon, W. C. K. *Faraday Discuss.* **1999**, *112*, 13.
(52) Kaji, K.; Nishida, K.; Kanaya, T.; Matsuba, G.; Konishi, T.; Imai, M. *Adv. Polym. Sci.* **2005**, *191*, 187.
(53) Muthukumar, M. *Adv. Polym. Sci.* **2005**, *191*, 241.
(54) Cavagna, A.; Attanasi, A.; Lorenzana, J. *Phys. Rev. Lett.* **2005**, *95*, 115702.
(55) Gagne, C. J.; Gould, H.; Klein, W.; Lookman, T.; Saxena, A. *Phys. Rev. Lett.* **2005**, *95*, 095701.
(56) Shinbrot, T.; Muzzio, F. J. *Nature* (*London*) **2001**, *410*, 251.
(57) Gollub, J. P.; Langer, J. S. *Rev. Mod. Phys.* **1999**, *71*, S396.
(58) Debenedetti, P. G. *Nature* (*London*) **2006**, *441*, 168.
(59) Hunter, C. A.; Sanders, J. K. M. *J. Am. Chem. Soc.* **1990**, *112*, 5525.
(60) Kostorz, G., Ed. *Phase Transformations in Materials*; Wiley-VCH: New York, 2001.
(61) Hoffman, J. D.; Davis, G. T.; Lauritzen, Jr., J. I., In *Treatise on Solid State Chemistry*; Hannay, N. B., Ed.; Plenum Press: New York, 1976; Vol. *3*, Chapter 7.
(62) Hoffman, J. D.; Lauritzen, J. I., Jr. *J. Res. Natl. Bur. Std.* **1960**, *64A*, 73.
(63) Prausnitz, J. M.; Lichtenthaler, R. N.; de Azevedo, E. G. *Molecular Thermodynamics of Fluid-Phase Equilibria*, 3rd ed.; Prentice-Hall: Upper Saddle River, NJ, 1998.
(64) Witten, T. A. *Rev. Mod. Phys.* **1999**, *71*, S367.
(65) Frenkel, D. *Physica A* **1999**, *263*, 26.
(66) Snir, Y.; Kamine, R. D. *Science* **2005**, *307*, 1067.
(67) Liu, A. J.; Nagel, S. R. *Nature* (*London*) **1998**, *396*, 21.
(68) Trappe, V.; Prasad, V.; Cipelletti, L.; Segre, P. N.; Weitz, D. A. *Nature* (*London*) **2001**, *411*, 772.
(69) Lois, G.; Blawzdziewicz, J.; O'Hern, C. S. *Phys. Rev. Lett.* **2008**, *100*, 028001.
(70) Lee, H. N.; Paeng, K.; Swallen, S. F.; Ediger, M. D. *Science* **2009**, *323*, 231.
(71) Weitz, D. A. *Science* **2009**, *323*, 214.